EnMAP Flight Campaigns
Technical Report

Omongwa Salt Pan, Namibia

Robert Milewski, Holger Eichstaedt, Maximilian Brell,
Robert Behling, Sabine Chabrillat

Recommended citation of the report:

Milewski, Robert; Eichstaedt, Holger; Brell, Maximilian; Behling, Robert; Chabrillat, Sabine (2020): Omongwa Salt Pan, Namibia 2015 - An EnMAP Preparatory Flight Campaign. EnMAP Flight Campaigns Technical Report, GFZ Data Services.
DOI: https://doi.org/10.2312/enmap.2020.005

The data described in this report:

Milewski, Robert; Eichstaedt, Holger; Brell, Maximilian; Behling, Robert; Chabrillat, Sabine (2020): Omongwa Salt Pan, Namibia 2015 - An EnMAP Flight Campaign, GFZ Data Services.
DOI: https://doi.org/10.5880/enmap.2020.005

Imprint

EnMAP Consortium

Helmholtz Centre Potsdam
GFZ German Research Centre for Geosciences

Publisher
GFZ Data Services

Telegrafenberg
D-14473 Potsdam
December 2020

DOI: https://doi.org/10.2312/enmap.2020.005

EnMAP Flight Campaigns
Technical Report

Omongwa Salt Pan, Namibia

Robert Milewski[1], Holger Eichstaedt[2], Robert Behling[1], Maximilian Brell[1], Sabine Chabrillat[1]

[1] *GFZ German Research Centre for Geosciences*

[2] *dimap Group*

Table of Contents

1. Abstract

The dataset is composed of Neo HySpex (VNIR/SWIR) hyperspectral imagery acquired during the GFZ/DIMAP Geoarchive airborne campaign on June 6th, 2015 covering the Omongwa salt pan located in the South-West Kalahari, Namibia. The dataset includes 9 merged cloud-free flight lines with 408 spectral bands ranging from VNIR to SWIR wavelength regions (0.4-2.5 µm). The dataset also includes Level 2A EnMAP-like imagery simulated using the end-to-end Simulation tool (EeteS). The overall goal of the campaign was to test the potential of advanced optical hyperspectral remote sensing, or imaging spectroscopy, for the analysis of surface processes in the Omongwa salt pan and for the quantification of surface sediments. Specifically, the mineralogical composition of exposed evaporites such as halite, gypsum and calcite were investigated at the airborne and spaceborne scale, associated with comprehensive field campaigns, ich which spectral reflectance and ground-truth chemical data of field samples have been collected. The data are highly novel and can be used as testbeds for the development and validation of retrieval algorithms based on air- and space-borne hyperspectral imagery for estimation of surface sediment properties in a highly saline and dynamic environment.

Center coordinates 23.69 S / 19.38 E

Keywords: Hyperspectral Imagery, imaging spectroscopy, spaceborne, playa, salt pan, saline, mineralogy, salts, evaporite minerals, gypsum content

Key references:

This dataset has been used in several studies:

Milewski, R., Chabrillat, S., Behling, R., 2017. Analyses of Recent Sediment Surface Dynamic of a Namibian Kalahari Salt Pan Based on Multitemporal Landsat and Hyperspectral Hyperion Data. Remote Sensing 9, 170. https://doi.org/10.3390/rs9020170

Milewski, R., Chabrillat, S., Brell, M., Schleicher, A.M., Guanter, L., 2019. Assessment of the 1.75 µm absorption feature for gypsum estimation using laboratory, air- and spaceborne hyperspectral sensors. International Journal of Applied Earth Observation and Geoinformation 77, 69–83. https://doi.org/10.1016/j.jag.2018.12.012

Milewski, R., Chabrillat, S., Bookhagen, B., 2020. Analyses of Namibian Seasonal Salt Pan Crust Dynamics and Climatic Drivers Using Landsat 8 Time-Series and Ground Data. Remote Sensing 12, 474. https://doi.org/10.3390/rs12030474

An overview of the EnMAP mission is provided in Guanter et al. (2015):

Guanter, L., Kaufmann, H., Segl, K., Foerster, S., Rogaß, C., Chabrillat, S., …, and Sang, B. (2015). The EnMAP spaceborne imaging spectroscopy mission for earth observation. Remote Sensing, 7(7), 8830-8857. https://doi.org/10.3390/rs70708830

1 Introduction

The Environmental Mapping and Analysis Program (EnMAP) is a German hyperspectral satellite mission that aims at monitoring and characterizing the Earth's environment on a global scale. EnMAP serves to measure and model key dynamic processes of the Earth's ecosystems by extracting geochemical, biochemical and biophysical parameters, which provide information on the status and evolution of various terrestrial and aquatic ecosystems. In the frame of the EnMAP preparatory phase and in the frame of related projects such as in this study, airborne campaigns including airborne and in-situ measurements in different environments are being conducted. The main purpose of these campaigns is to support the development of scientific applications for EnMAP. In addition, the acquired data are input in the EnMAP end-to-end simulation tool (EeteS) and are employed to test data pre-processing and calibration-validation methods. The campaign data are made freely available to the scientific community under a Creative Commons Licence CC BY 4.0 Licence. An overview of all available data is provided in a specifically developed metadata portal on the project website (http://www.enmap.org/data_tools/flights/).

1.1 Flight Campaign "Omongwa Pan, Namibia 2015"

The natural depression of the Omongwa Pan is located in the southwestern Kalahari (23°41.4 S, 19°22.6 E), approximately 260 km southeast of Windhoek, Namibia (Figure 1). The Omongwa Pan is classified as salt pan or playa, due to its surface that features seasonal to ephemeral inundation events and subsequent drying and build-up of evaporite-rich sediments. The Omongwa pan covers an area of 3 by 5 km, which makes it the largest in a group of regional pans that are developed in calcretes of a paleodrainage system. The pan surface is mainly vegetation-free and consists of unconsolidated and evaporite rich sediments with a high range and dynamic in exposed surface mineralogical mixtures of halite, gypsum, calcite, and clay minerals (e.g. sepiolite). Hyperspectral imagery (HySpex VNIR/SWIR) was acquired in June 2015 combined with comprehensive field surveys throughout different seasons between 2014 – 2016 to explore applications of hyperspectral imagery regarding the analysis of surface mineralogy of potential dust source regions and highly dynamic landscape features.

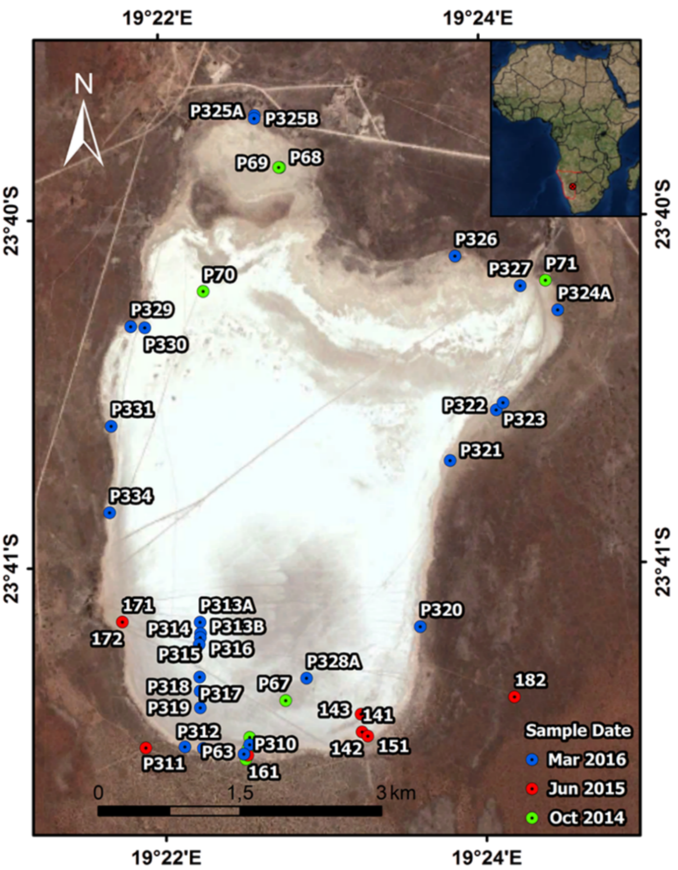

Figure 1. Omongwa pan and sample location (Basemap source: DigitalGlobe RGB image, September 2013, provided by Google Inc. (Mountain View, CA, USA)) (Milewski et al. 2019).

2 Data Acquisition

The airborne datasets were obtained at an altitude of 2850 m above ground level over the Omongwa pan on June 6th, 2015 during a GFZ/DIMAP airborne campaign (http://dimap-spectral.com/) in the frame of the BMBF-SPACES collaborative project Geoarchives - Signals of Climate and Landscape Change preserved in Southern African Geoarchives. The hyperspectral data have been acquired using two Neo HySpex cameras in 9 flight stripes with alternating SE/NW heading under blue sky conditions at 10:30-12:00 UTC with a sun elevation angle of 40-45° and sun azimuth angle of -10° to +20°. The NEO HySpex system consists of two push-broom hyperspectral cameras (VNIR-1600 operating over the 0.4 1.0 µm and SWIR-320m e operating over 1.0 2.5 µm range) with a total of 408 wavebands and a spectral resolution of 3.7 nm (VNIR-1600) and 6.0 nm (SWIR-320m e) (Norsk Elektro Optikk 2017). The original ground sampling distance (GSD) of the image captured was 1.2 m for the VNIR spectrometer (flown without field of view expander) and 2.4 m for the SWIR-320m-e camera (flown with field of view expander). The higher spatial resolution and consequent smaller swath width of the VNIR sensor coverage resulted in narrow stripes of missing VNIR information of about 5% between flight lines shown in Fig. 2.

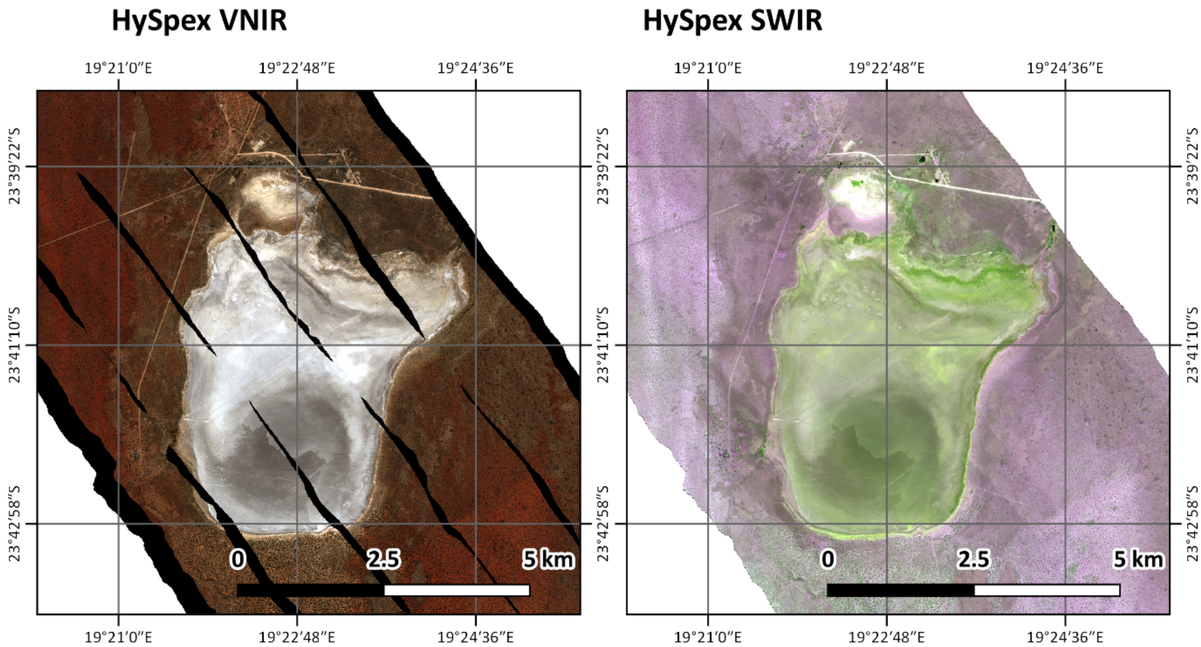

Figure 2: Overview of the HySpex data visualized as VNIR and SWIR color composite. Left: true color RGB composite (0.65, 0.55, 0.45 µm), right: false color RGB composite (1.75, 1.12, 2.22 µm).

Simultaneously with the hyperspectral VNIR-SWIR data acquisition, a digital elevation model and thermal hyperspectral imagery were acquired with the LMS-Q780 long-range airborne laser scanner and with the Telops Hyper-Cam LWIR camera, respectively. The Hyper-Cam LWIR data were acquired with 4 m spatial resolution and 4 cm^{-1} spectral resolution covering the spectral range 7.7-11.7 µm. These two datasets can be made available on request.

3 Data Processing and Products

The acquired HySpex data were radiometrically corrected using sensor specific software of the instrument manufacturer. Further processing from at sensor radiance to orthorectified surface reflectance was realized with the GFZ in-house processing chain HyPrepAir based on the sensor models and the simultaneously measured IMU/GPS data stream (Brell et al. 2016). In a first step, physically based atmospheric correction of the HySpex data was carried out in sensor geometry for the separated VNIR and SWIR sensors with the ATCOR-4 software (Richter and Schläpfer 2016) based on the radiative transfer model MODTRAN 5 (Richter and Schläpfer 2002). A desert aerosol model, water vapour column of 1.0 g m^{-2}, and a visibility of 60 km, were selected as atmospheric parameters. Spectral smile could be detected and removed using the ATCOR-4 smile detection routine. In a second step, a direct geometric correction was realized. The VNIR sensor was used as a reference to co-register the SWIR sensors automatically based on a ray tracing procedure (Brell et al. 2016). Thus, the SWIR spectra are implemented and adapted to the overlapping VNIR spectra wavelength. Then the flight stripes were composed into a single mosaic with a spatial resolution of 2.4 m without image feathering or colour balancing to keep the original data values. To further remove atmospheric attenuation and spectral artefacts an Empirical Line Calibration (ELC) (Aspinall et al., 2002) implemented in ENVI 5.3 (Harris Geospatial Solutions 2015) was performed using field-measurements of several reflectance targets with different albedo acquired simultaneously to the overflight (Milewski et al. 2019).

Simulated EnMAP L2A data products in reflectance geocorrected were generated using the EnMAP end-to-end simulation software (Segl et al. 2012), resulting in a simulated hyperspectral data cube at 30m spatial resolution with 242 bands.

HySpex
Bands: 408
Wavelengths: 414.6 – 2492.8

EnMAP
Bands: 242
Wavelengths: 423.0 – 2438.6

Table 1: Overview of the two hyperspectral imaging airborne mosaics

Dataset	Flight Altitude	Flight Heading	Solar Azimuth	Solar Zenith	Pixel Size	Lines
HySpex Omongwa mosaic	2850 m	SE/NW, NW/SE	-10° to +20°	~40-45°	2.4 m	3593
EnMAP simulated Omongwa mosaic	N/A	SE/NW	-10° / -20°	~40-45°	30 m	341

4 File Description

4.1 File Format

Envi Image File [*.bsq] and descriptive header file [*.hdr] for the remote sensing data. Excel file [*.xlsx] for the additional soil database.

4.2 Data content and structure

Image files are described in the header file by the following attributes: ENVI description, samples, lines, bands, header offset, file type, data type, interleave, sensor type, byte order, map info, wavelength units, band names, wavelength, fwhm (full width half maxima).

The Excel table containing the soil / sediment database includes the following attributes: Sample ID, geographic coordinates, Munsell soil color, texture (clay, sand, silt fractions), organic carbon content, pH, XRD minerology (quartz, halite, gypsum, calcite) and ASD FieldSpec 3 laboratory reflectances.

5 Data Quality

5.1 Airborne HySpex data

Due to the campaign date in southern hemispherical winter (June), the illumination conditions were non-optimal which results in a relatively low signal-to-noise ratio (SNR). Additionally, the VNIR data coverage is incomplete with about 5% data missing between flight stripes.

5.2 Spaceborne EnMAP simulation

The quality of the simulated EnMAP data is related to the quality of the HySpex data that the simulation was based on. Missing VNIR data coverage has been interpolated using neighboring pixel information on the 30 m ground sampling distance basis.

6 Additional Data

In addition to the airborne survey, comprehensive surface samples have been collected during three field campaigns that took place on 14-16 October 2014, 4-6 June 2015 and 3-5 March 2016 at the Omongwa pan. The location and date of the field sampling is shown in Figure 1. A total of 46 top surface crust (<2 cm) samples were collected in homogeneous areas, that were subsequently analysed in the laboratory for chemical and spectral reflectance properties.

6.1 Wet chemistry data

The resulting database includes mineralogical XRD analysis and the sedimentary properties color, texture, organic carbon content and pH. Initial sample preparation comprised of sub-sampling and drying at 105 °C. After the removal of organic material and carbonates using 10% H_2O_2 and 17% HCl, respectively, sample texture was determined by a combination of wet-sieving (particles > 63 µm) and sedimentation (particles < 63 µm). pH was measured in a 0.01 M $CaCl_2$ suspension. Mineral characterization was carried out using a PANalytical Empyrean powder X-ray diffractometer (XRD) with a theta-theta-goniometer, Cu-Kα radiation (λ = 0.15418 nm), automatic divergent and anti-scatter slits and a PIXcel3D detector. Diffraction data were recorded from 4.5° to 85° 2Θ with a step-size of 0.0131 and a step time of 60 s. The generator settings were 40 kV and 40 mA. All samples were crushed and powdered to a grain size of <63 µm. These samples were used for the qualitative and quantitative mineral analysis. A few samples were also powdered to <10 µm, but no strong differences in intensities were observed. The qualitative phase composition was determined using the software DIFFRAC.EVA (Bruker), and the quantitative mineralogical composition of the samples (in weight %) was calculated using a Rietveld based method implemented in the program AutoQuan (GE SEIFERT; (Taut, Kleeberg, and Bergmann 1998). More detailed information on the field campaigns, soil sampling and chemical analyses can be found in Milewski et al., 2017, 2019.

6.2 Spectral reflectance data

Laboratory spectral reflectance of the 46 bulk sediment samples were measured using an ASD FieldSpec, which provides reflectance data at 1 nm interval and a range of 350 – 2500 nm under controlled environmental and illumination conditions simulating spaceborne observations (sensor nadir viewing, light source azimuth 35°). A spectral library associated with the optical signatures of the samples was created after correcting for detector offset and averaging 5 measurements per target.

7 Dataset Contact

Robert Milewski
Email: robert.milewski@gfz-potsdam.de
Phone: +49 (0) 331 288 1187

Sabine Chabrillat
Email: chabri@gfz-potsdam.de
Phone: +49 (0) 331 288 1108

8 Acknowledgements

This research was supported by the German Federal Ministry of Education and Research (BMBF) as part of the joint project "GeoArchives—Signals of Climate and Landscape Change preserved in Southern African GeoArchives" (No. 03G0838A) within the "SPACES Program—Science Partnerships for the Assessment of Complex Earth System Processes" research initiative. Further support was received from the EnMAP science preparatory program funded under the DLR Space Administration with resources from the German Federal Ministry of Economic Affairs and Energy (grant number: DLR/BMWi 50 EE 1348). We would also like to thank Daniel Berger from GFZ Potsdam for help with the field work and the XRD analysis, as well as Hartmut Liep and Marina Ospald for sample preparation. The authors also wish to thank Klaus-Dieter Hanemann and the DIMAP team for their investment in a successful airborne survey, and Karl Segl for performing the EnMAP image simulation.

9 References

Aspinall, R.J., Marcus, W.A., Boardman, J.W., 2002. Considerations in collecting, processing, and analysing high spatial resolution hyperspectral data for environmental investigations. J Geograph Syst 4, 15–29. https://doi.org/10.1007/s101090100071

Brell, M., Rogass, C., Segl, K., Bookhagen, B., Guanter, L., 2016. Improving Sensor Fusion: A Parametric Method for the Geometric Coalignment of Airborne Hyperspectral and Lidar Data. IEEE Transactions on Geoscience and Remote Sensing 54, 3460–3474. https://doi.org/10.1109/TGRS.2016.2518930

Guanter, L., Kaufmann, H., Segl, K., Foerster, S., Rogass, C., Chabrillat, S., Kuester, T., Hollstein, A., Rossner, G., Chlebek, C., Straif, C., Fischer, S., Schrader, S., Storch, T., Heiden, U., Mueller, A., Bachmann, M., Mühle, H., Müller, R., Habermeyer, M., Ohndorf, A., Hill, J., Buddenbaum, H., Hostert, P., van der Linden, S., Leitão, P.J., Rabe, A., Doerffer, R., Krasemann, H., Xi, H., Mauser, W., Hank, T., Locherer, M., Rast, M., Staenz, K., Sang, B., 2015. The EnMAP Spaceborne Imaging Spectroscopy Mission for Earth Observation. Remote Sens 7, 8830–8857. https://doi.org/10.3390/rs70708830

Milewski, R., Chabrillat, S., Behling, R., 2017. Analyses of Recent Sediment Surface Dynamic of a Namibian Kalahari Salt Pan Based on Multitemporal Landsat and Hyperspectral Hyperion Data. Remote Sensing 9, 170. https://doi.org/10.3390/rs9020170

Milewski, R., Chabrillat, S., Brell, M., Schleicher, A.M., Guanter, L., 2019. Assessment of the 1.75 µm absorption feature for gypsum estimation using laboratory, air- and spaceborne hyperspectral sensors. International Journal of Applied Earth Observation and Geoinformation 77, 69–83. https://doi.org/10.1016/j.jag.2018.12.012

Richter, R., Schläpfer, D., 2016. Atmospheric / Topographic Correction for Satellite Imagery (ATCOR-2/3 User Guide, Version 9.0.2, March 2016). URL: http://www.rese.ch/pdf/atcor3_manual.pdf (last access 18 December 2020)

Richter, R., Schläpfer, D., 2020. Atmospheric / Topographic Correction for Airborne Imagery (ATCOR-4 User Guide, Version 7.3.0, March 2020). https://www.rese-apps.com/pdf/atcor4_manual.pdf (last access 18 December 2020)

Segl, K., Guanter, L., Rogass, C., Kuester, T., Roessner, S., Kaufmann, H., Sang, B., Mogulsky, V., Hofer, S., 2012. {EeteS—The} {EnMAP} {End-to-End} Simulation Tool. {IEEE} {J-STARS} 5, 522–530. https://doi.org/10.1109/JSTARS.2012.2188994

Taut, T., Kleeberg, R., Bergmann, J., 1998. Seifert Software: The new Seifert Rietveld program BGMN and its application to quantitative phase analysis. Materials Structure 5, 57–66. URL: https://citeseerx.ist.psu.edu/viewdoc/download?doi=10.1.1.566.5481&rep=rep1&type=pdf (last access 18 December 2020)